

Structural and Optical Properties of Aluminum Doped Cadmium Oxide (CdO:Al) Thin Film Prepared by Sol-Gel Spin-Coating Method

Madihazaman Syeda* Moniruzzaman Syed**, Jessica Massey**, Karstan Harvey**, Miara Hurd**, Jolaikha Sultana*** and Md Farhan Azim***

*Department of Bio-medical engineering, University of Memphis, Memphis, TN, USA

Email: rhymesyeda@gmail.com

**Division of Natural and Mathematical Sciences, LeMoyne-Owen College, Memphis, TN, USA

Email: moniruzzaman_syed@loc.edu

***Department of Physics and Material Science, University of Memphis, Memphis, TN, USA

Email: jsltana1@memphis.edu

Abstract

Aluminum-doped cadmium oxide (CdO:Al) thin films are deposited on silica substrates by the sol-gel spin-coating method as a function of spin coater's rpm (revolution per minute). Cadmium acetate dihydrate and Aluminum nitrate have been taken as the precursor material and a source of Al-dopant respectively. CdO:Al thin films are characterized by Raman scattering, x-ray diffraction (XRD), Fourier Transform Infrared (FT/IR), Field emission scanning electron microscopy (FE-SEM), SEM-EDX, UVvis, AFM, Ellipsometer and Four-point probe. XRD result indicates the highest crystallinity at 6000 rpm with a crystallite size of 31.845 nm, cubic phase formation, and strain of $\sim 1.6 \times 10^{-2}$. FE-SEM/SEM/EDX shows the well-faceted homogeneous surface structure at 6000 rpm having the average particle size of 130.05 nm, lowest resistivity of $9 \times 10^{-8} \Omega\text{-cm}$ and the lowest band gap energy of 2.19 eV. FT/IR confirms the presence of CdO:Al in the film with the peak position shifting to higher wavenumbers at higher rpm. Raman results indicate that the presence of crystalline phase located at 933.93 cm^{-1} .

Keywords- Cadmium oxide, FE-SEM, Raman and Sol-gel process

1. Introduction

Transparent Conducting Oxides (TCOs) have been attracted as a semiconducting material for variety of applications in optical, thermal, electronic and solar energy devices^[1]. Considering high conductivity and transparency in the visible region, ZnO^[2-5], SnO₂^[6] and CdO^[7-8] are playing very important materials. Because of low optical bandgap energy, CdO thin film is not showing popular TCO materials; however, it is a semiconducting oxide with extraordinary carrier mobility, simple crystal structure and nearly metallic conductivities^[9] has displayed a great potential for optoelectronic devices^[10-11]. Due to a great reflectance in the infrared region, along with high transparency in the visible region, it has been employed as heat mirrors^[9]. The high conductivity of the films has been manipulated for fabricating highly efficient, large-area solar cells. It has been reported the effects of various dopant like Indium (In), Tin (Sn) and Fluorine (F) on CdO^[12]. Aluminum (Al) is a good dopant on ZnO thin films, however, no report has been found on Al-doped CdO thin films. CdO thin films prepared by various methods such

as activated reactive evaporation [13], solution growth [14], spray pyrolysis [15], rf-sputtering [16], MOCVD [17] and PLD [18]. In this paper, Aluminum-doped cadmium oxide (CdO:Al) thin films have been synthesized on low-cost silica substrates by the sol-gel spin-coating method as a function of spin coater's rpm (revolution per minute). CdO:Al thin films are characterized by Raman, x-ray diffraction (XRD), Fourier Transform Infrared (FT/IR), Field emission scanning electron microscopy (FE-SEM), SEM-EDX, AFM, Four-point probe and Ellipsometer.

II. Experimental Method

A. Sol-gel Preparation

The Aluminum doped Cadmium Oxide thin films were fabricated on silica substrate by the sol-gel spin-coating method, using the precursor material, cadmium acetate dehydrate ($\text{CH}_3\text{COO})_2\text{Cd}\cdot 2\text{H}_2\text{O}$) and Aluminum Nitrate ($\text{Al}(\text{NO}_3)_3\cdot 9\text{H}_2\text{O}$) as the Aluminum doped source. Primarily, 3.99 grams of cadmium acetate was measured and mixed with 25 mL of Isopropyl alcohol for 0.3 M solution (Fig. 1). For aluminum (Al) doping, 5.6 grams of Aluminum Nitrate was mixed with the above solution. Resultant solution was stirred with magnetic stirrer at 70°C for 1 hour. After the solution was fully homogeneous, the pH was measured to approximately ~ 3 by adding 2 mL of acetic acid incrementally. The solution was kept at room temperature for a few days.

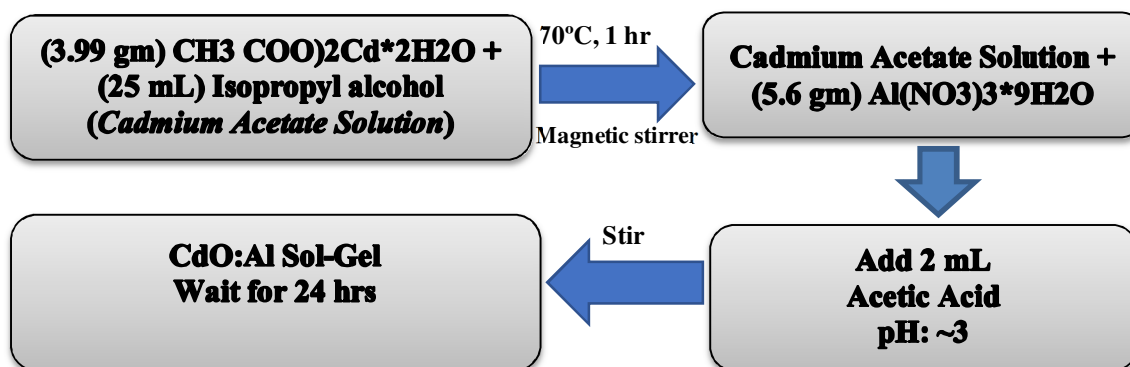


Fig. 1 shows CdO:Al sol-gel preparation process

B. Film Deposition

Fig. 2 shows the SPI KW-4AD (two stage-spinning) spin coater used in this experiment. The 927 diaphragm vacuum pump is connected with the spin coater in order to hold the substrate tightly on the vacuum-chuck. Due to precise dispensing of precursor-liquid uniformly onto substrate, a liquid dispenser is used. Nitrogen (N_2) gas cylinder as a back pressure is connected to the liquid dispenser. Sol-gel liquid holder is also connected to it with a stand just above the spin coater chuck as shown in Fig.2. With adjusting the back pressure, the amount of precursor liquid (~ 0.1 ml) can be dispersed on the substrate. Fused quartz silica substrates were cutting with the dimension of 10 mm x 5 mm and 5mm x 5 mm for different measurements. The substrates were cleaned for 15 min using acetone, 15 min using ethanol and 15 min using deionized (DI) water in an ultrasonic cleaner and dry-out with N_2 gun. The Spin-coater was then calibrated to begin the deposition process. The spin coater has attached 2-steps speed control dials. For the first step, the spinning time and rpm values kept constant as 9 sec and 1000 respectively. The second step, the

spinning time was fixed as 10 sec and rpm was changing from 1000, 2000, 3000, 4000, 5000 and 6000. After the first deposition, samples were annealed at 185°C for 15 minutes to evaporate the moisture. For the second layer, the samples were then placed back into the spin-coater and deposit the layer using the same above parameters and heated at 185°C again. For the third and final layer, samples were annealed at 400°C for 1 hour. The samples were then cooled and stored for characterizations.



Table I: Deposition Conditions of CdO:Al thin film growth

<i>Parameters</i>	<i>Quantity</i>
$(\text{CH}_3\text{COO})_2\text{Cd}\cdot 2\text{H}_2\text{O}$	3.99 gm
$\text{Al}(\text{NO}_3)_3\cdot 9\text{H}_2\text{O}$	5.6 gm
Isopropyl Alcohol	25 mL
Acetic acid	2mL
Growth time (Stage2) (constant)	10 sec
Stage1 rpm and time (constant)	1000 & 9 sec
<i>rpm (stage2)variable</i>	<i>1000-6000</i>
Spun sol-gel	0.1 mL
Substrate	Silica
Annealing temperature	400 °C, 1 hr

Fig. 2 shows the Spin-Coater used in this experiment

C. Thin Film Characterizations

Structural characterization was analyzed by X-Ray Diffraction (XRD), Scanning Electron Microscopy (SEM), Atomic Force Microscopy (AFM), Raman Scattering, Fourier-transformed infrared spectroscopy (FT/IR), Surface Topography, and Surface Roughness. The Raman spectra of the films were measured using a portable iRaman (B&W TeK) with the argon ion laser having an excitation wavelength of 514 nm and the power was less than 5 mW. The device used for surface topography was the DTX Digital Microscope: Levenhuk: Zoom & Joy. The surface roughness device used was the Mitytoyo Surface roughness scanning machine. X-Ray Diffraction scanning is a tool used to analyze the structure, composition, and properties of materials to the atomic level. The structure can be scanned to identify characterize and quantify the crystalline phases and structures in a material. XRD scanning can also test to find certain elements, the stress level, scattering angles and texture analysis within a sample. Scanning Electron Microscopy is used to scan samples using electrons instead of light to form images. SEM can evaluate materials for surface flaws, fractures, contaminants, corrosion, and analyze crystalline structures. Atomic Force Microscopy (AFM) uses a sharp tip to measure and visualize materials at the atomic and nano-scales. AFM measures various surfaces, localizing at different points and forces. AFM can also measure adhesion strength, magnetic forces, and mechanical properties. Raman Scattering is an optical process where incoming light interacts with a sample and produces scattered light that is lessened in energy by the vibrational mode of the chemical bonds in the sample. It gives information about the vibrations with a molecule and rotational energy in gases. FT/IR uses an analytical technique that uses infrared light to scan samples and monitor the chemical properties and displays a spectrum. Surface topography uses the film thickness and roughness ratio, scanning the surface both in its profile shape and surface roughness taking microscopic images of the surface. Surface roughness measured the texture of the sample. A stylus top makes direct contact with the surface of a sample and detects the motion of the stylus.

III. Results and Discussion

A. Structural Characterization measuring with Surface Topography

The samples were scanned by the surface topography DTX Digital Microscope showing the grouping and heterogeneous distributions (Samples: a-d) of the CdO:Al thin films to the uniform distributions. (Samples: e-f). This result is consistent with AFM result which explains below.

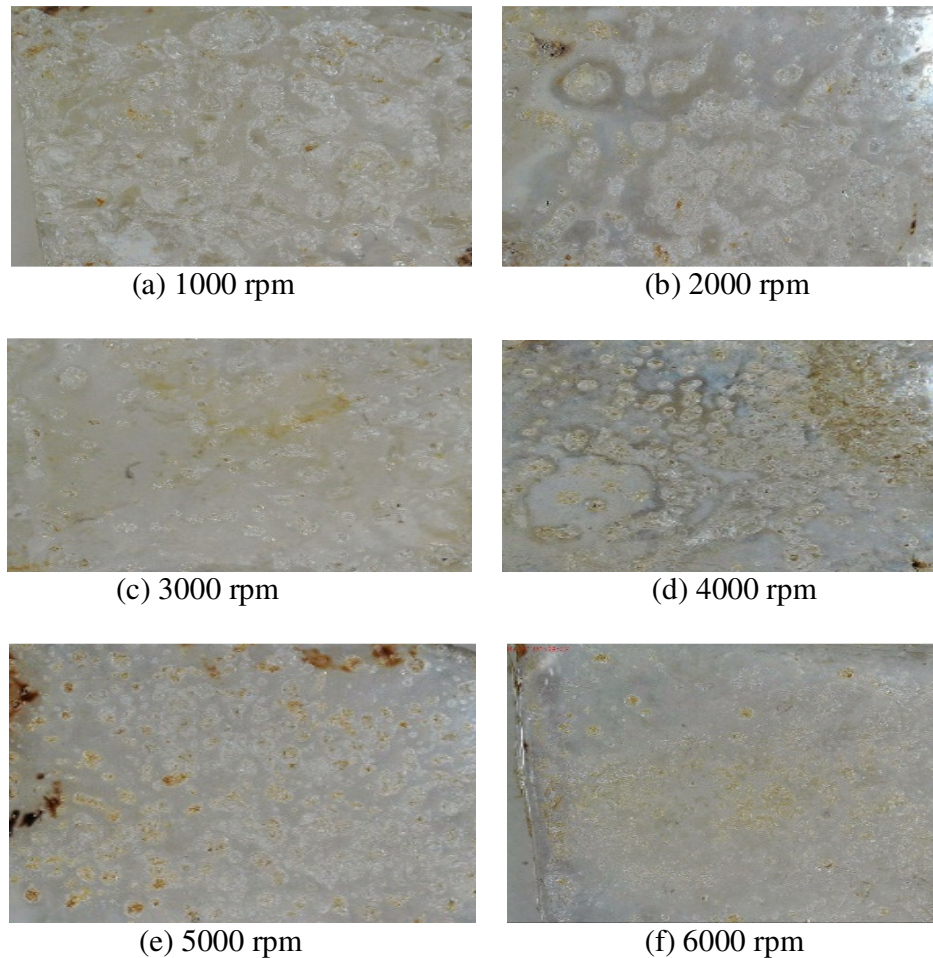


Fig. 3 shows surface morphology of CdO:Al thin film as a function of rpm: (a) 1000, (b) 2000, (c) 3000, (d) 4000, (e) 5000 and (f) 6000, respectively

B. Structural Characterization by XRD

The crystallographic properties of prepared thin films were investigated using an XRD instrument Bruker D8 Advance diffractometer (Bruker, Germany) with Cu K α ($\lambda \sim 1.54 \text{ \AA}$) radiation in $2\theta \sim 20^\circ - 70^\circ$, scan rate 0.2 mm/sec and 0.0484 step size. The average crystallite size, $[\delta]$, was estimated from the Full width half maximum (β) of the XRD spectra using Scherrer's formula as follows:

$$[\delta] = k\lambda/\beta\cos\theta \quad (1)$$

where k , λ , β and θ are a constant, shape factor value as 0.9, the wavelength of X-ray (1.54 Å), the full width at half maximum (FWHM) and Bragg angle of the diffraction peak respectively.

The typical XRD pattern of CdO:Al thin film is shown in Fig. 4. For all films, the characteristic peaks were identified as (1 1 1), (2 0 0), (2 2 0), (311) and (222) originated at the 2θ values 38.17°, 38.8°, 44.97°, 45.17° and 64.82° respectively. Results indicate the cubic phase formation of all films prepared as a function of rpm.

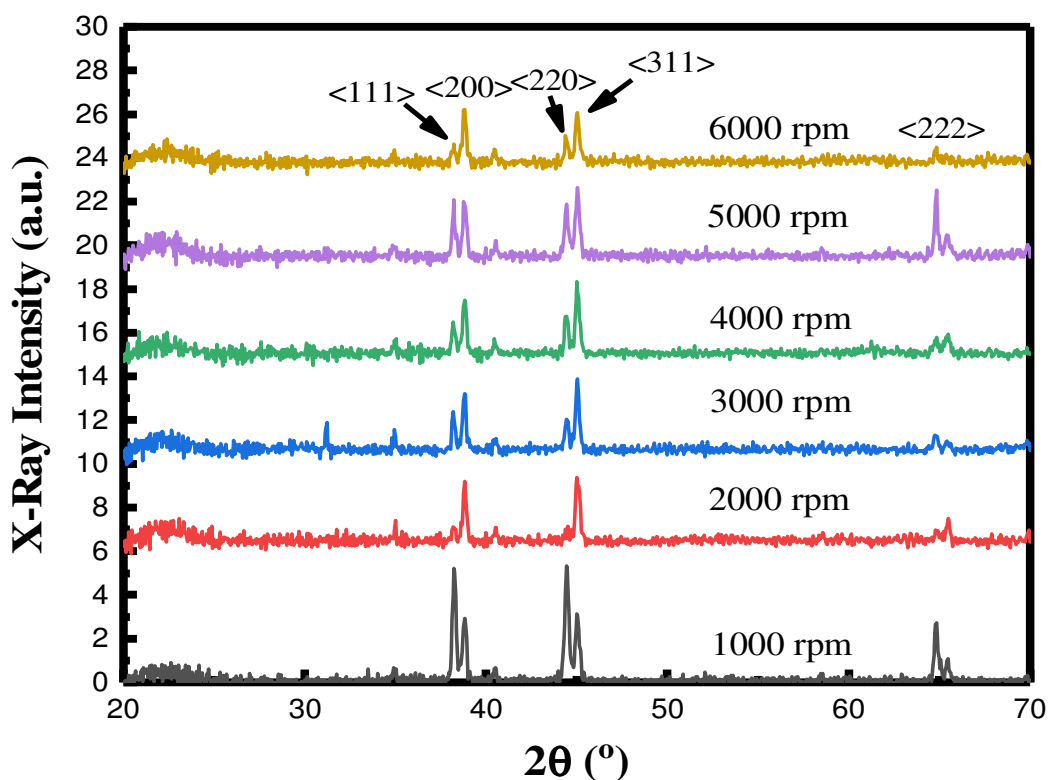


Fig. 4 shows XRD spectra of CdO:Al thin films as a function of various rpm

Fig. 5(a) shows XRD crystallites size (δ) values of CdO:Al thin film as a function of rpm. It is indicated that δ increases with increasing rpm. Maximum δ was estimated by 30.91 nm at 6000 rpm. As shown in Fig. 5(b), The XRD intensity decreases with increasing rpm and opposite relationship was observed for FWHM with rpm. Fig. 5 (c) represents a $\beta_T \cos\theta$ as function of $4\sin\theta$ (W-H plot) of CdO:Al thin film. The slope of the straight line provides the strain of $\sim 1.6 \times 10^{-2}$.

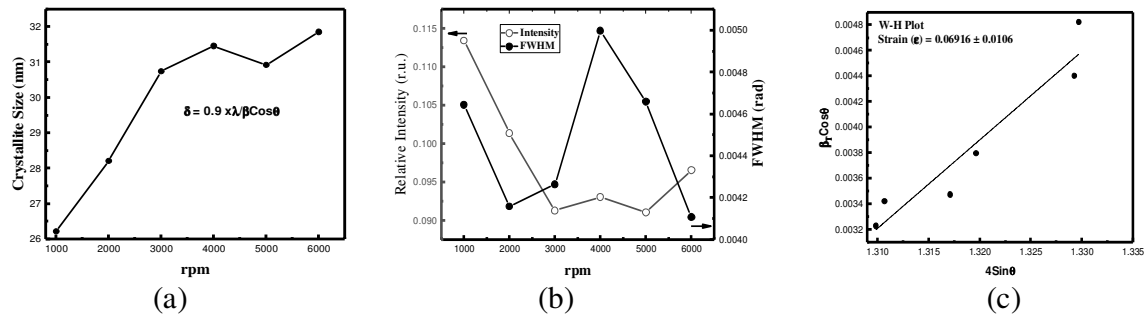


Fig.5 (a) crystallite size, (b) relative intensity and FWHM and (c) W-H plot of CdO:Al as a function of rpm

C. Structural Characterization using Raman scattering

Raman spectroscopy is the study of the interaction between light and matter. In this process, light is inelastically scattered. This is called the Raman Effect. Photons of a single wavelength in the visible range which would be light of a single color are focused onto a sample. Most commonly a laser is used as it is a powerful monochromatic source. The photons interact with the molecules and are either reflected, absorbed, transmitted or scattered. Using Raman spectroscopy, we study the scattered photons. Fig.6 shows, the comparison of Raman data for CdO:Al thin films under two different rpm values of 1000 and 6000 respectively. Raman excitation line at 935 cm^{-1} for 1000 rpm and 933 cm^{-1} for 6000 rpm were observed. Results indicate a strong correlation between vibrational and electronic properties (peak positions, width, and relative intensity) of advanced doped-oxide materials. It is indicated that peak position shifted toward the lower wave number for the film at higher rpm values which is also showing the highest crystallite size as shown in Fig. 5(a).

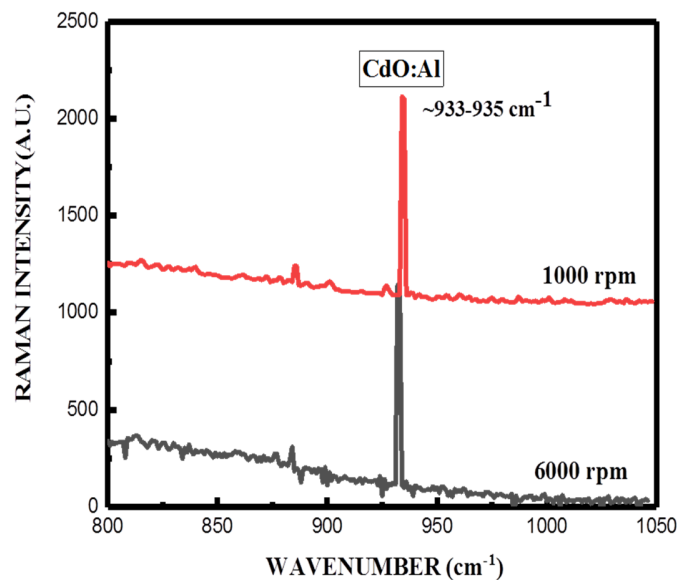


Fig. 6 shows the Raman Spectra for CdO:Al thin films under 1000 and 6000 rpm

D. Structural Characterization using FT/IR

Fig. 7 shows the bonding properties of CdO:Al thin films by FTIR in the range of 400 to 1500 cm^{-1} at different rpm values. Spectrum of the CdO:Al thin films exhibit a strong, broad absorption band at 490–550 cm^{-1} corresponds to the formation of CdO:Al bonds. The significant amount of H₂O and carbonaceous (CO) materials are also present at ~900–1100 cm^{-1} and ~750 – 850 cm^{-1} respectively in all films. With increasing the rpm values, the CdO:Al broad bands are found to be sharpened.

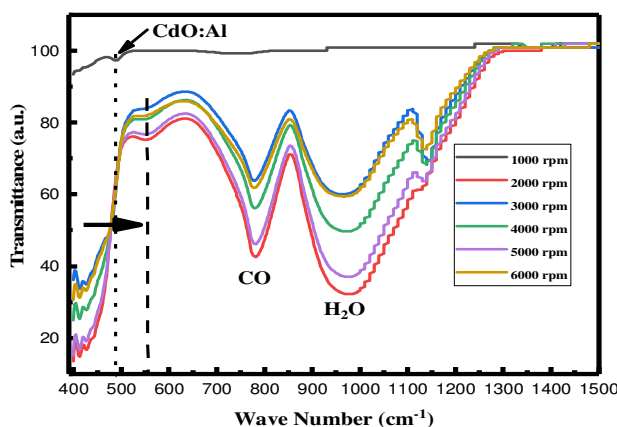


Fig. 7 shows the FT/IR of CdO:Al thin film as a function of various rpm

Fig.8(a) shows that CdO:Al band peaks position as a function of various rpm values. Results indicate that the peaks position shifted towards the higher wave number at higher rpm values above 1000 rpm and stays constant as shown below. This result is consistent with Raman and XRD measurements. Fig. 8(b) shows the absorbance of CdO:Al thin film as a function of rpm values.

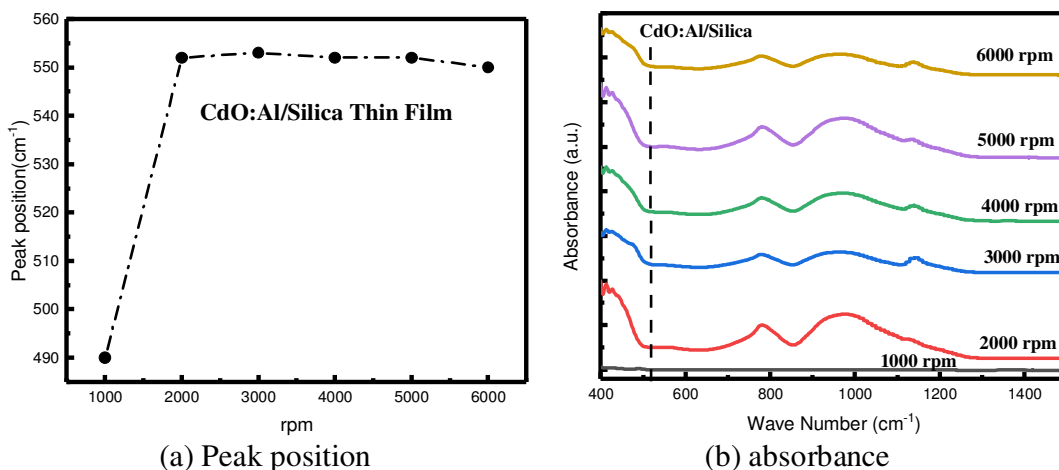


Fig. 8 shows (a) peak position and (b) absorbance of CdO:Al thin film as a function of rpm

E. Structural Characterization using Field Emission-Scanning Electron Microscopy (FE-SEM)

Fig. 9 shows the surface microstructures of CdO:Al thin films using FE-SEM analysis are compared under two different rpm values of 1000 (Fig.9a) and 6000 (Fig.9b), respectively. CdO:Al thin films are heterogeneous in nature. For 1000 rpm, it is seen that the particles are irregular spherical in shape together with some large patches. However, for 6000 rpm, the enhanced surface uniformity with improved particle size distributions, more regular shapes and the highest agglomerations were observed.

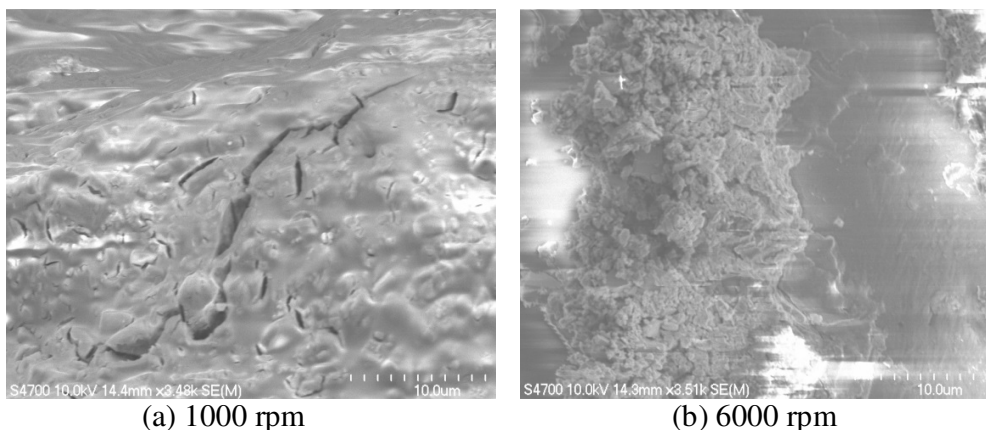


Fig. 9 FE-SEM micrographs of CdO:Al thin film under (a) 1000 rpm and (b) 6000 rpm

Fig. 10 shows the average particle size distribution of CdO:Al thin film measured from the corresponding FE-SEM images and are plotted as histogram graphs under two different rpm values of 1000 and 6000 respectively.

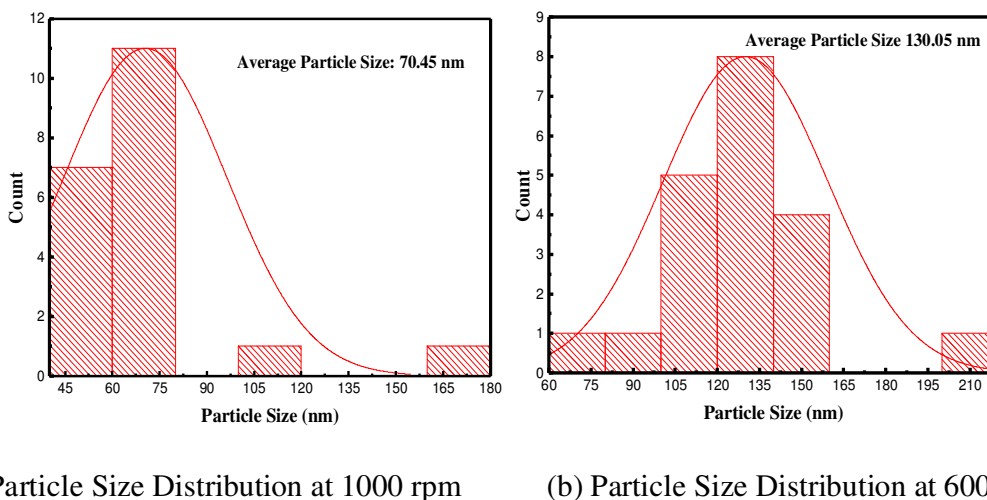


Fig. 10 Average particle sizes of CdO:Al thin film obtained by histogram images (a) 1000 rpm and (d) 6000 rpm

The average particle sizes of CdO:Al thin films are 70.45 nm and 130.05 nm for 1000 rpm and 6000 rpm, respectively. The particle size calculated from FE-SEM greater when compared with the particle size calculated from XRD, because symmetrical reflection like XRD determines the

coherence length due to lattice atoms of crystalline materials whereas the surface probes like FE-SEM estimates the agglomerated structures on the surface of the film^[19].

Fig. 11 shows typical EDX spectrum of CdO:Al thin film under 1000 rpm and 6000 rpm. It shows the presence of Cd, O and Al for both films along with some signals from silica substrates. The percentage of elements (at%) observed are shown below.

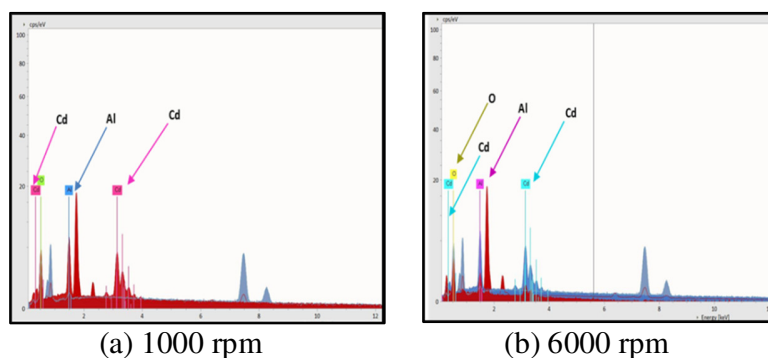


Fig. 11 Typical EDX spectrum of CdO:Al thin film (a) 1000 rpm [Cd (36.21 at%), O(53.94 at%) and Al(9.8 at%)] and (b) 6000 rpm [Cd (56.21 at%), O(46.21 at%) and Al(9.21 at%)]

F. Structural Characterization using Surface Roughness

Fig. 12 shows the R_a and d as a function of rpm values. R_a values were measured by Mitutoyo SurfTest SJ-310 portable surface roughness tester with the scanning speed of 0.5 mm/s. Film thickness were measured by FS-RT300 Multi-Wavelength Ellipsometer System.

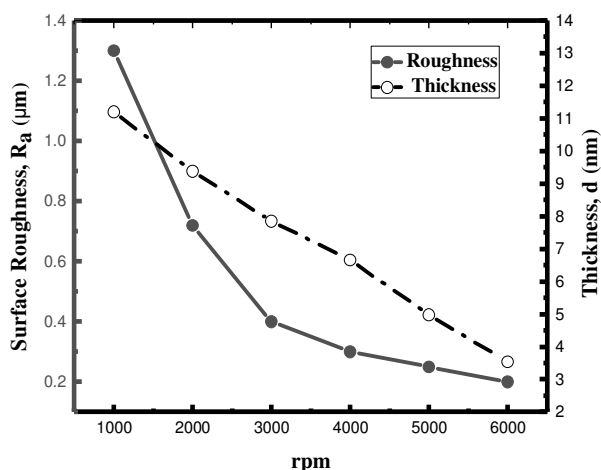


Fig. 12 Surface Roughness (R_a) and film thickness (d) of CdO:Al thin films with various rpm

As revealed in this diagram, d decreases as rpm increases. On the other hand, R_a values are found to be decreased with the increment of rpm values. Smoother surface has observed with the lowest d value of 3.5 nm at 6000 rpm, which has also given the highest crystallinity. This result is perfectly consistent with the XRD measurement as shown in Fig. 5(a).

G. Optical characterizations using Ellipsometry

Fig. 13 shows the refractive index (n) and dielectric constant (κ) of CdO:Al thin films as a function of rpm. From this diagram, it is seen that κ of the films increased as rpm increases. Maximum κ has found to be 9.5 at 6000 rpm. On the other hand, n decreases as rpm increases having the lowest value of 1.2. The reason for this increment in dielectric constant with rpm is expected to result from film densification and proper nucleation processes on the silica substrate having the highest crystallinity of the film.

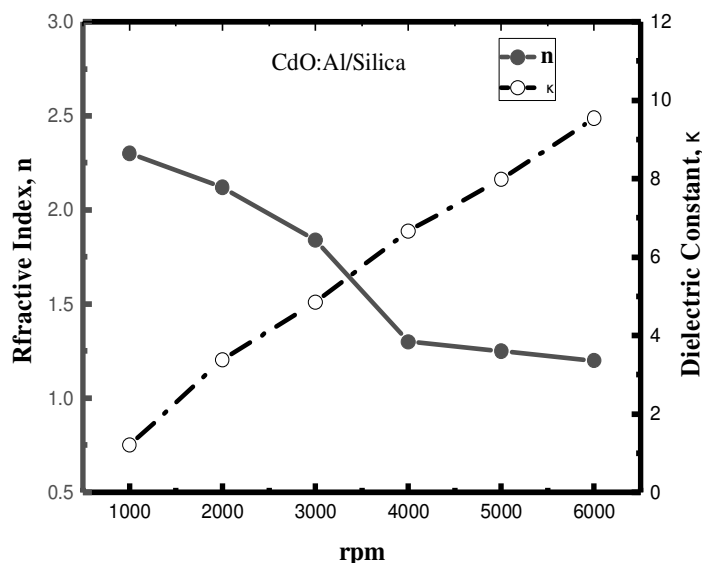


Fig. 13 shows the refractive index (n) and dielectric constant (κ) of CdO:Al thin film as a function of rpm

H. Electrical characterizations using Resistivity Analysis

Fig. 14 shows the variation of resistivity of CdO:Al thin films as a function of rpm. The resistivity, ρ, of the films was calculated by

$$\rho = \frac{\pi V}{\ln 2 I} \tag{2}$$

where v and I are voltage and current respectively.

From this figure, it is seen that the resistivity decreases with increasing the rpm. The resistivity is measured for an electric field of 1MV/cm. The electrical resistivity of film decreases with an increase in rpm. The lowest resistivity of CdO:Al thin film has found $9 \times 10^{-8} \Omega\text{-cm}$. at 6000 rpm which is showing the highest crystallinity as shown in Figs. 3-6.

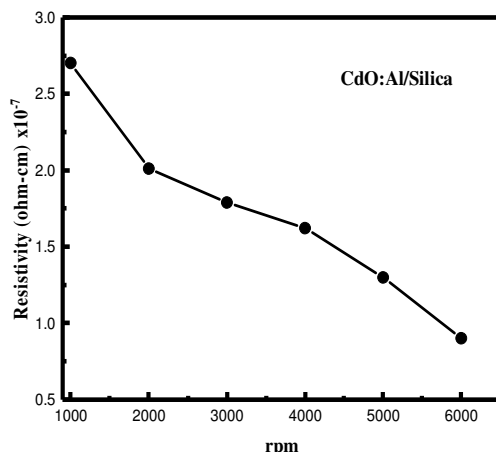


Fig. 14 The variation in resistivity of the CdO:Al thin films as a function of rpm

I. Optical characterizations using UV-vis Analysis

Fig. 15 shows the band gap energy (E_g) with the various rpm values. E_g was estimated by using absorption spectra for CdO:Al thin films in the wavelength range of 200-800 nm. It shows that the E_g decreases with increase in rpm from 2.68 -2.19 eV. It suggests that higher rpm decrease the transparency due to increased absorption by free electrons ^[20].

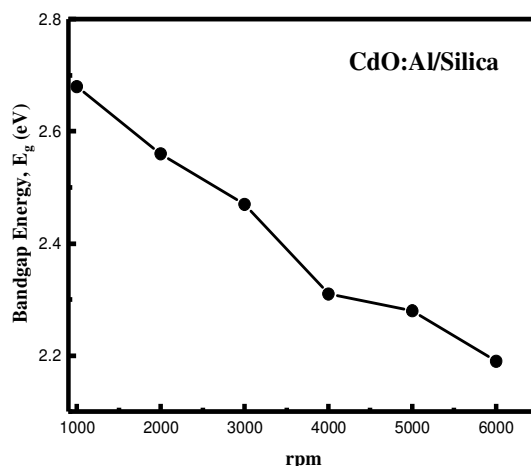


Fig 15 shows the variation of band gap energy of CdO:Al thin films as a function of rpm

J. Surface morphological characterizations using AFM

Fig. 16 shows the surface roughness of CdO:Al thin films by AFM under two different conditions of 1000 rpm and 6000 rpm. The root mean square roughness (R_{rms}) for 1000 rpm is approximately 39.45 nm and for 6000 rpm is 29.89 nm observed. This result is consistent with the result in Fig. 3. The light colored areas in the micrographs represented an agglomeration of grains and the white areas are the clusters that were formed as neighboring grains can combine with each other ^[21]. The decrease in surface roughness with the higher rpm is related to the increment in the films grain size as shown in Fig. 5a.

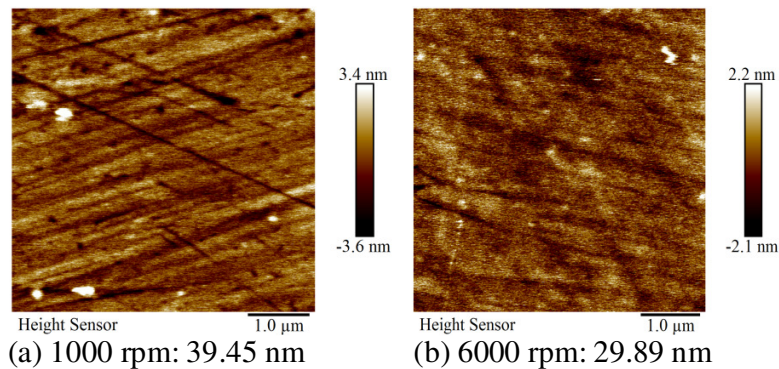


Fig. 16 2D-AFM images of CdO:Al thin films under (a) 1000 rpm and (b) 6000 rpm

IV. CONCLUSIONS

CdO:Al thin film have successfully been deposited on silica substrates as a function of various rpm values using the Sol-Gel Spin Coating method. XRD result indicates the highest crystallinity at 6000 rpm with a crystallite size (δ) of 31.845 nm, strain of $\sim 1.6 \times 10^{-2}$ and also a proper cubic phase formation. Raman scattering results indicate the peak position (pp) located at 933 cm^{-1} which is confirming the presence of crystalline structure, and it is also observed that pp shifted to the lower wave number at higher rpm. FT/IR confirms the presence of CdO:Al in all films at $\sim 500 \text{ cm}^{-1}$, with the higher rpm the peak position shifting towards the higher wavenumbers. FE-SEM shows the well-faceted homogeneous structure having the average particle size of 130.05 nm at 6000 rpm. EDX analysis is confirming the presence of Cd, O and Al elements in the films. Film thickness and surface roughness (R_a) have been found decreasing with increasing rpm. This result is consistent with the AFM result where the lowest R_{rms} has been estimated by 29.89 nm at 6000 rpm. Maximum κ has found by 9.5 and the lowest value of n has found by 1.2 at 6000 rpm. The lowest resistivity has observed of $9 \times 10^{-8} \Omega\text{-cm}$ at 6000 rpm, which is showing the highest crystallinity of the film. Optical study shows that the band gap energy (E_g) has estimated by 2.19 eV at 6000 rpm.

Acknowledgement

The authors would like to thank Department of Education (LeMoyne-Owen College, MSEIP Grant #P120A220064) for the support during this work. Special thanks to the Department of Physics, University of Memphis, TN for XRD measurement and the department of chemistry, Villanova University, PA for Raman measurement.

REFERENCES

- [1] Ramakrishna, K. T. Reddy, Shanthini G.M., Johnson D., and Miles R. W., Thin solid Films, P:427, 397 (2003)
 - [2] M.S. Tokumoto, A. Smith, C.V. Santilli, S.H. Pulcinelli, A.F. Craievich, E. Elkaim, A. Traverse, V. Briois, Thin Solid Films 416 (2002) 284.
 - [3] K. Matsubara, P. Fons, K. Iwata, A. Yamada, K. Sakurai, H. Tambo, S. Niki, Thin Solid Films 431–432 (2003) 369.
 - [4] K.L. Chopra, S.R. Das, Thin Film Solar Cells, Plenum Press, New York, 1983 ch. 3, p. 346.
 - [5] S. Major, A. Banerjee, K.L. Chopra, Thin Solid Films 143 (1986) 19.
 - [6] K.L. Chopra, S. Major, D.K. Pandya, Thin Solid Films 102 (1983) 1.
 - [7] M. Yan, M. Lane, C.R. Kannewurf, R.P.H. Chang, Appl. Phys. Lett. 78 (2001) 2342.
 - [8] A.J. Verkey, A.F. Fort, Thin Solid Films 239 (1994) 211.
- Acknowledgement
- [9] R. J. Deokate, A. V. Pawar and S. M. Moholkar, V. S. Sawant, and Pawar C. A., Appl. Surf. Sci., 254 (7), 2187 (2008)
 - [10] M. Yan, M. Lane, C.R. Kannewurf, R.P.H. Chang, Appl. Phys. Lett. 78 (2001) 2342.
 - [11] B.J. Lewis, D.C. Paine, Mater. Res. Soc. Bull. 25 (2000) 22.
 - [12] P.K. Ghosh, R. Maity, K.K. Chattopadhyay, Sol. Energy Mater. Sol. Cells 81 (2004) 279
 - [13] G. Phatak, R. Lal, Thin Solid Films 245 (1994) 17.
 - [14] A.J. Verkey, A.F. Fort, Thin Solid Films 239 (1994) 211.

- [15] G. Sanatana, M. Acevedo, O. Vigil, F. Cruze, G. Contreras-puente, L. Vaillant, *Superficies y Vacío* 9 (1999) 300.
- [16] N. Ueda, H. Meada, H. Hosono, H. Kawazoe, *J. Appl. Phys.* 84 (1998) 6174.
- [17] A.J. Freeman, K.R. Poepelmeier, T.O. Mason, R.P.H. Chang, T.J. Marks, *Mater. Res. Soc. Bull.* 25 (2000) 45.
- [18] M. Yan, M. Lane, C.R. Kannewurf, R.P.H. Chang, *Appl. Phys. Lett.* 78 (2001) 2342.
- [19] B. Shaha, R. Thapa and K.K. Chattopadhyay, *Solid State Commun.*, 2008, **145**, 33-37.
- [20] X. Wu, T.J. Coutts, W. P. Mulligan, *J. Vac. Sci. Technol.* A15 (1997) 1057
- [21] Akyuz. I, Kose S, Ketenci E, Bilgin V, Atay F. Optical, structural and surface characterization of ultrasonically sprayed CdO:F films, *Journal of Alloys and compounds*, **509** (9), 1947-1952 (2011)